Laterally-coupled dual-grating distributed feedback lasers for generating mode-beat Terahertz signals

Lianping Hou[1,*], Mohsin Haji[2], Iain Eddie[3], Hongliang Zhu[4], John H. Marsh[1]

[1]*School of Engineering, University of Glasgow, Glasgow, G12 8LT, U.K.*
[2]*National Physical Laboratory, Teddington, Middlesex, TW11 0LW, U.K.*
[3]*CST Global Ltd., 4 Stanley Blvd, Blantyre, Glasgow, G72 0BN U.K.*
[4]*Institute of Semiconductors, No. A35, East Qinghua Road, Haidian District, Beijing 1000083, P.R. China*
**Corresponding author: lianping.hou@glasgow.ac.uk*

We present a laterally-coupled dual wavelength 1.56/1.57 μm AlGaInAs/InP DFB laser, which, by introducing of two different grating periods on each sidewall, emits two longitudinal modes simultaneously within the same cavity at a frequency separation of 0.82 THz. The beating signal is stabilized by nonlinear four-wave mixing in an electroabsorption modulator (EAM), located within a monolithically integrated resonant cavity. A stable 0.82 THz beating signal was observed over a wide range of bias parameters in terms of drive currents and bias to the DFB and EAM sections.

OCIS codes: 140.5960, 140.3490, 300.3700, 300.2570.

THz radiation is of increasing importance for a variety of new applications, such as medical imaging, remote sensing, and THz communications [1-2]. One of the techniques used to generate optical THz signals is by photomixing beams from two different distributed feedback (DFB) lasers [3, 4] or alternatively using an extended cavity configuration [5]. Dual mode lasers (DML) utilising integrated distributed Bragg reflectors (DBR) or DFB laser cavities have also been used [6, 7]. A much simpler DML source for pumping, capable of uncooled operation and with a simple device structure is strongly desired. Among the various reported DML configurations, simultaneous emission of two longitudinal modes within the same cavity is very appealing because the device is compact, gives a stable beat frequency with high spectral quality, can be manufactured at low cost and is straightforward to package [8].

DMLs operating in the 1.5 μm telecommunications window for silica fibre are most desirable. At this wavelength a plethora of components has been developed to modulate, control and manipulate optical signals, and erbium doped fibre amplifiers (EDFAs) can be used to increase the signal power to hundreds of Watts if required.

Here we report, for the first time, a 1.56 μm DML with two longitudinal modes lasing simultaneously within the same cavity separated by 0.82 THz. Both modes are affected by much the same electrical, thermal and mechanical fluctuations, also known as the common-mode-noise rejection effects [3]. The frequency difference between the modes is determined essentially by each side of the laterally-coupled grating structures, and crucially not by the ambient temperature or injection current (of course, a small difference frequency shift will appear due to fluctuations of temperature and injection current). An additional resonator, containing an electroabsorption modulator (EAM) in which four-wave mixing (FWM) takes place, locks the phase of the two optical signals. In contrast to the complex fabrication processes used for conventional DFB lasers, those based on laterally-coupled gratings offer advantages such as regrowth-free fabrication and the associated flexibility in design. The grating can be simultaneously lithographically patterned and etched along with the ridge waveguide, significantly simplifying the device manufacturing process. The

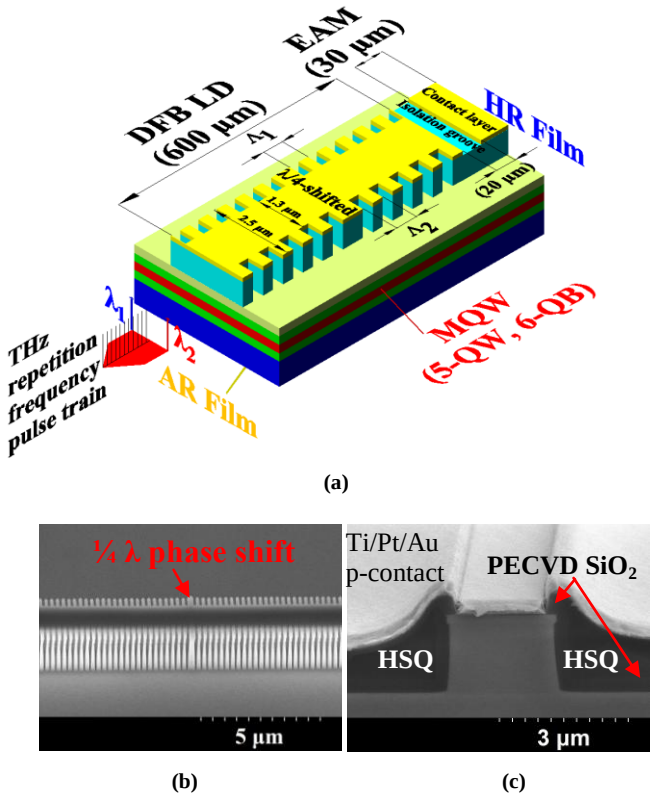

Fig. 1. (a) Schematic of the device, (b) SEM picture of the first-order 50% duty cycle sidewall gratings with a 0.6 μm recess and λ/4 shift, (c) SEM picture of the cross-section of the EAM.

regrowth-free approach enables Al-containing epitaxial layers to be used, as there is no exposure of surfaces containing Al, which can oxidize and cause problems during epitaxial regrowth [9]. The results presented in this paper suggest that our device could be used as a practical compact, stable, solid-state laser source for generating THz radiation using a photoconductive antenna [3] or nonlinear optical crystal [10].

A schematic of the fabricated device along with its dimensions is shown in Fig. 1(a). The device comprises an EAM section (30 µm), a DFB section (600 µm) with an electrical isolation slot (20 µm) between them. The ridge waveguide is 2.5 µm wide and 1.92 µm high, and the effective index of the guided mode is estimated, using numerical simulation, to be 3.20.

The epitaxial structure used for the device is based in the AlGaInAs/InP material system and contains five active QWs and six quantum barriers (QB), and was previously in [11]. The EAM section, the HR coating on its output facet, and the DFB gratings form a cavity that is resonant at both DFB wavelengths. This cavity is used to enhance coupling between the two longitudinal modes, to improve phase locking and stabilize the mode beating frequency through the mechanism of FWM in the EAM [12]. The DFB laser has a cavity length of 600 µm. The gratings are of first-order with a 50% duty cycle and formed by etching 0.6 µm recesses into the sidewalls of the waveguide, as shown in Fig. 1(b). The periods of the gratings on each side of the ridge are 244 nm (Λ_1) and 245 nm (Λ_2), which select Bragg wavelengths of λ_1 (1561.60 nm) and λ_2 (1568.3 nm) respectively. The separation of the wavelengths is 6.70 nm, and the corresponding beating frequency is 820 GHz. Quarter wavelength shifts were inserted at the middle of the DFB laser gratings to ensure each line oscillated in a single longitudinal mode (see Fig. 1(b)). The coupling coefficient κ for devices with identical gratings on both sides of the ridge was measured to be approximately 80 cm^{-1} using the sub-threshold spectral fitting method. The 20 µm long electrical isolation section between the DFB and EAM sections is formed by removing the semiconductor contact layer.

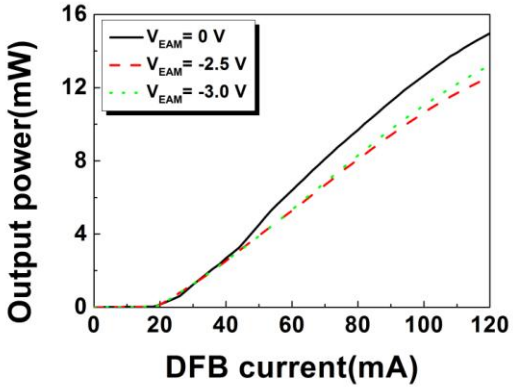

Fig. 2. Measured output power from DFB side as a function of I_{DFB} for different V_{EAM}.

The device fabrication processes are similar to those described in [13], i.e., negative tone Hydrogen Silsequioxane (HSQ) was used as an e-beam lithography resist and reactive ion etching (RIE) dry etching hard mask, as well as a material for planarizing the 1.92 µm high ridge waveguide and gratings (see Fig.1 (c)) [14]. As can be seen in Fig. 1(b), the mask transfer of the grating into the upper cladding layers is excellent, with good sidewall verticality, and little RIE lag at the foot of the gratings. As a final step, the sample was cleaved into individual laser bars with the facets at the DFB end of the device anti-reflection (AR) coated (<0.05%) and the EAM facets high-reflection (HR) coated (92%). The devices were mounted epilayer-up on a copper heat sink on a Peltier cooler. The heat sink temperature was set at 20 °C and the devices were tested under CW conditions.

Figure 2 shows typical light-DFB current (L-I_{DFB}) characteristics from the DFB output side with different reverse bias voltages (V_{EAM}) applied to the EAM. The threshold current and output facet slope efficiency with a 0 V applied to the EAM section were 18 mA (1.2 kA/cm^2) and 14.7% W/A, respectively, values that are comparable to those of traditional molecular beam epitaxy (MBE) grown, buried ridge structure, AlGaInAs/InP DFB lasers [15]. When the EAM reverse voltage was increased from 0 V to -2.5 V, the threshold current was unchanged but the

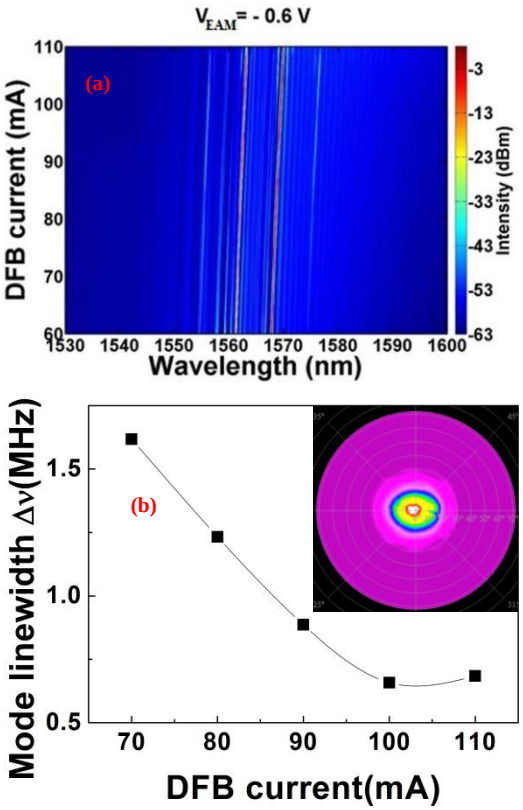

Fig. 3. (a) Wavelength map as a function of I_{DFB} for V_{EAM} = -0.6 V, (b) measured beating linewidth vs I_{DFB} for V_{EAM} = -0.6 V; the inset shows the 2-D FFP at I_{DFB} =100 mA.

slope efficiency reduced as a result of increased absorption. With further increases of the EAM reverse voltage, the DFB laser became optically isolated from the HR reflector and the slope efficiency increased, with the threshold current still unchanged. This indicates that the DFB laser was working as an independent cavity and the partitioning electrical slot prevented electrical coupling between the DFB and EAM sections.

A beating signal was observed when the DFB section was forward biased and the EAM section was either left floating or had a reverse bias applied. For the reverse voltage applied to the EAM section in the range -1.0 V $\leq V_{EAM} \leq$ -0.3 V , the beating signal was more stable and the autocorrelation (AC) used to observe and monitor the pulse train indicated strong coherence. This is ascribed to FWM in the EAM [12] maintaining a good phase relationship between the two fundamental modes. The DFB wavelengths λ_1 and λ_2 and their spacing were accurately determined by Λ_1 and Λ_2, respectively. The temperature tuning coefficient of λ_1 and λ_2 was <0.06 nm/K in the range 20°C - 70°C, and so the mode spacing was in effect independent of temperature.

Stable beating over a wide range of electrical drive parameters is also a key feature of this laser, with stable THz mode beating observed for -1.0 V $\leq V_{EAM} \leq$ -0.3 V and 60 mA $\leq I_{DFB} \leq$ 110 mA. For -0.3 V < $V_{EAM} \leq$ 0 V and -2.0 V $\leq V_{EAM} <$ -1.0 V, the beating signal was less clear, and coherence was poor for V_{EAM} < -2.0 V . These results confirmed the importance of FWM in the EAM section – in the bias range -1.0 V $\leq V_{EAM} \leq$ -0.3 V, increasingly strong mixing took place, similarly to [12]. As the bias voltage was made more negative than -1.5 V, the absorption of the EAM was so large and the cavity Q so low, the HR was effectively isolated from the DFB section, the modes were no longer locked and the FWM peaks were no longer visible in the optical spectrum, as discussed in more detail below.

Figure 3(a) shows a 2D optical spectral plot for the most stable beating range of I_{DFB} from 60 mA to 110 mA with V_{EAM} = -0.6 V. The spectrum was measured with a resolution bandwidth (RBW) of 0.07 nm. The laser shows two stable longitudinal modes with a mode spacing of around 6.7 nm. The inclusion of a quarter wavelength shift in the middle of the cavity for each grating meant that mode-hopping was suppressed. As I_{DFB} was increased, the two main wavelengths were red-shifted at the same rate of 0.04nm/mA due to heating. The mode spacing was constant over all stable bias conditions, confirming variations in the operating wavelengths of the laser resulting from tuning the DFB current do not compromise the beat tone.

Due to the high repetition frequency of the beat signal, it was not possible to perform a direct measurement of the radio frequency (RF) characteristics. However, we were able to infer these characteristics by using the well-known coherent heterodyne technique to measure the optical linewidth of individual modes when the laser was driven to operate over ideal beating conditions. The experimental RF spectra can be approximated as having a Lorentzian profile, which means the optical spectral linewidth primarily comes from the spontaneous emission of the intrinsic linewidth of the laser itself [16]. The technical noise, such as mechanical vibrations, temperature fluctuations and injection current noise can be neglected [16]. Figure 3(b) shows the measured beat mode linewidth as a function of I_{DFB} for V_{EAM}= -0.6 V. Here, we note the trend that the beat mode linewidth reduces as I_{DFB} is increased. The narrowest observed linewidth of about 700 kHz was achieved at I_{DFB}= 100 mA. In contrast, a separate measurement of a counterpart single grating DFB laser emitting a single longitudinal mode fabricated in the same wafer has a typical optical linewidth of 3.5 MHz at the same current

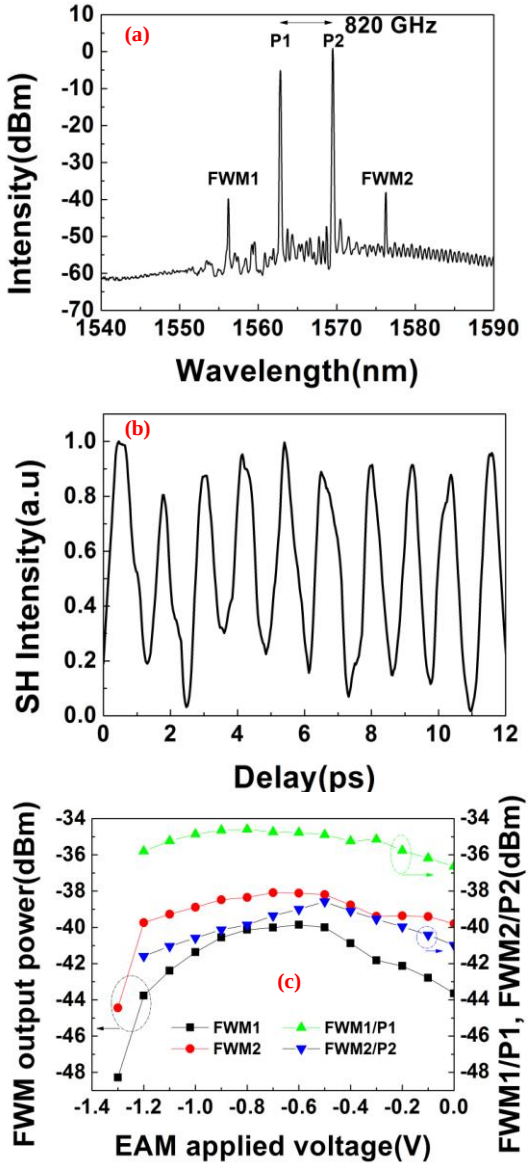

Fig.4.(a)Optical spectrum and (b) measured autocorrelation pulse train for I_{DFB}=100 mA and V_{EAM}= -0.6 V. (c) FWM output power and ratio to the corresponding lasing power vs the EAM applied voltage.

injection level. This reduction of the linewidth provides strong evidence that in the beating regime, the two modes are indeed mutually phase-locked.

The far field pattern (FFP) from the DML was measured with high resolution (0.9º). The inset in Fig. 3(b) shows the 2D FFP measured at I_{DFB} = 100 mA and V_{EAM}= -0.6 V. The beam is almost circular (34° × 35°) and is indistinguishable to that expected from the fundamental mode of the ridge waveguide, confirming both of the lasing wavelengths are in the fundamental *TE* mode. Moreover, when displacing an optical fiber along the transversal horizontal direction (//) closely approaching the DFB output facet while scanning I_{DFB} and V_{EAM}, the measured optical spectrum is not sensitive to the fiber position.

Figure 4(a) shows the optical spectra of the DFB laser at an injection current of 100 mA with V_{EAM} = -0.6 V. The measured lasing modes were at wavelengths of 1562.8 (peak P1) and 1569.5 nm (peak P2), corresponding to a difference frequency of 820 GHz, with a side mode suppression ratio (SMSR) >42 dB. The values of P1 and P2 differ because of the gain spectrum of the material. The FWM sidebands at 1556.2 (peak FWM1) and 1576.3 nm (peak FWM2) can be clearly seen. The 15 dB power enhancements of the sidebands above the cavity modes indicate good phase stability between the two main modes [6]. In a practical THz system, the sidebands would not affect photomixing, as their power is, in turn, about 35 dB below the two main lasing modes. The corresponding measured AC trace is shown in Fig. 4(b), which indicates a sinusoidal modulation with some fluctuations in the peak intensity, which are due to the finite resolution of the autocorrelator system and technical noise that stems from the measurement system itself. The average period of the measured emitted pulse train was 1.22 ps, which corresponds to the expected repetition frequency of 820 GHz, and is in agreement with the optical spectrum mode spacing shown in Fig. 4(a). Fig. 4(c) shows the dependence of the FWM output power on applied EAM voltage. As can be seen, FWM1 and FWM2 increased when V_{EAM} was changed from 0 V to -0.6 V, and then reduced when V_{EAM} <-0.6 V. The FWM signals were apparent until the bias on the EAM reached -1.4V, beyond which point no evidence of FWM could be seen in the optical spectrum. FWM1/P1, (the ratio of FWM1 to P1), and FWM2/P2, (the ratio of FWM2 to P2) follow the same trend. Fig. 4(c) confirms the key role that the EAM plays in terms of locking the phases of the two longitudinal modes [12].

In conclusion, a laterally-coupled, dual-wavelength DFB laser integrated with a nonlinear FWM cavity has been fabricated and characterized. The device emits two longitudinal modes simultaneously from within the same cavity, separated by 0.82 THz at a wavelength of around 1560 nm. The devices were fabricated using simple first-order sidewall grating technologies, which have the advantages of eliminating crystal regrowth and allowing the AlGaInAs quaternary structure to be used in the QW active section. The surface grating eliminates the need for complex regrowth fabrication steps normally associated with DFB lasers. Due to FWM in the resonant cavity, the device strongly favours operation in the mode-beating regime, with stable mode beating observed over a wide range of bias parameters in terms of drive current to the DFB and bias to the EAM. Compared with other reported DMLs, our laser uses a simple and reproducible fabrication technology and exhibits highly controllable and robust mode-beating operation. These laser diodes are expected to open up many opportunities for future compact THz applications.

This work was partly supported by the Royal Academy of Engineering Research Exchanges with China and India program under grant no 12/13RECI042.

References

[1] P. H. Siegel, IEEE Trans. Microw. Theory Tech. 50, 910 (2002).
[2] T. K. Ostmann, and T. Nagatsuma, J Infrared Milli Terahz Waves. **32**, 143 (2011).
[3] M. Tani, P. Gu, M. Hyodo, K. Sakai, and T. Hidaka, Optical and Quantum Electronics **32**, 503-520 (2000).
[4] I. S. Gregory, W. R. Tribe, C. Baker, B. E. Cole, M. J. Evans, L. Spencer, M. Pepper, and M. Missous, Appl. Phys. Lett. **86**, 204104 (2005).
[5] T. Kleine-Ostmann, P. Knobloch, M. Koch, S. Hoffmann, M. Breede, M. Hofmann, G. Hein, K. Pierz, M. Sperling, and K. Donhuijsen, Electron. Lett. **37**, 1461 (2001).
[6] A. Klehr, J. Fricke, A. Knauer, G. Erbert, M. Walther, R. Wilk, M. Mikulics, and M. Koch, IEEE J. Sel. Top. Quantum Electron. **14** (2), 289 (2008).
[7] N. Kim, J. Shin, E. Sim, C. W. Lee, D. S. Yee, M. Y. Jeon, Y. Jang, and K. H. Park, Opt. Express. **17**, 13851 (2009).
[8] F.Pozzi, R. M. De La Rue, and Marc Sorel, IEEE Photon. Technol. Lett. **18**, 2563(2006).
[9] H. Abe, S. G. Ayling, J. H. Marsh, R. M. De La Rue, and J. S. Roberts, IEEE Photon. Technol. Lett. **7**, 452 (1995).
[10] Z. Yang, L. Mutter, M. Stillhart, B. Ruiz, S. Aravazhi, M. Jazbinsek, A. Schneider, V. Gramlich, and P. Günter, Adv. Funct. Mater. **17**, 2018-2023 (2007).
[11] L. Hou, P. Stolarz, J. Javaloyes, R. Green, C. N. Ironside, M. Sorel, and A. C. Bryce, IEEE Photon. Technol. Lett. **21**, 1731 (2009).
[12] T. Mori and H. Kawaguchi, Appl. Phys. Lett., **85**, 869 (2004).
[13] L. Hou, R. Dylewicz, M. Haji, P. Stolarz, B. Qiu, A. C. Bryce, IEEE Photon. Technol. Lett. **22**, 1503 (2010).
[14] L. Hou, M. Haji, R. Dylewicz, B.C. Qiu, A. Catrina Bryc, IEEE Photon. Technol. Lett. **23**, 82(2011).
[15] M. Blez, C. Kazmierski, D. Mathoorasing, M. Quillec, M. Gilleron, H. Nakajima and B. Sennage, Electron. Lett. **27,** 93 (1992).
[16] S. Spiessberger , M. Schiemangk, A. Wicht, H. Wenzel, O. Brox, and G. Erbert, J. Lightwave Technol. **28**, 2611 (2010).

References with titles

[1] P. H. Siegel, "Terahertz technology", IEEE Trans. Microw. Theory Tech. 50, 910 (2002).

[2] T. K. Ostmann, and T. Nagatsuma, "A review on terahertz communications research", J Infrared Milli Terahz Waves. **32**, 143 (2011).

[3] M. Tani, P. Gu, M. Hyodo, K. Sakai, and T. Hidaka, "Generation of coherent terahertz radiation by photomixing of dual-mode lasers," Optical and Quantum Electronics **32**, 503-520 (2000).

[4] I. S. Gregory, W. R. Tribe, C. Baker, B. E. Cole, M. J. Evans, L. Spencer, M. Pepper, and M. Missous, "Continuous-wave terahertz system with a 60 dB dynamic range", Appl. Phys. Lett. **86**, 204104 (2005).

[5] T. Kleine-Ostmann, P. Knobloch, M. Koch, S. Hoffmann, M. Breede, M. Hofmann, G. Hein, K. Pierz, M. Sperling, and K. Donhuijsen, "Continuous-wave THz imaging", Electron. Lett. **37**, 1461 (2001).

[6] A. Klehr, J. Fricke, A. Knauer, G. Erbert, M. Walther, R. Wilk, M. Mikulics, and M. Koch, "High-power monolithic two-mode DFB laser diode for the generation of THz radiation", IEEE J. Sel. Top. Quantum Electron. **14** (2), 289 (2008).

[7] N. Kim, J. Shin, E. Sim, C. W. Lee, D. S. Yee, M. Y. Jeon, Y. Jang, and K. H. Park, "Monolithic dual-mode distributed feedback semiconductor laser for tunable continuous wave terahertz generation", Opt. Express. **17**, 13851 (2009).

[8] F.Pozzi, R. M. De La Rue, and Marc Sorel, "Dual-wavelength InAlGaAs–InP laterally coupled distributed feedback laser", IEEE Photon. Technol. Lett. **18**, 2563(2006).

[9] H. Abe, S. G. Ayling, J. H. Marsh, R. M. De La Rue, and J. S. Roberts, "Single-mode operation of a surface grating distributed feedback GaAs-AlGaAs laser with variable-width waveguide," IEEE Photon. Technol. Lett. **7**, 452 (1995).

[10] Z. Yang, L. Mutter, M. Stillhart, B. Ruiz, S. Aravazhi, M. Jazbinsek, A. Schneider, V. Gramlich, and P. Günter, "Large-size bulk and thin-film stilbazolium-salt single crystals for nonlinear optics and THz generation", Adv. Funct. Mater. **17**, 2018-2023 (2007).

[11] L. Hou, P. Stolarz, J. Javaloyes, R. Green, C. N. Ironside, M. Sorel, and A. C. Bryce, "Subpicosecond pulse generation at quasi-40-GHz using a passively mode locked AlGaInAs/InP 1.55 μm strained quantum well laser", IEEE Photon. Technol. Lett. **21**, 1731 (2009).

[12] T. Mori and H. Kawaguchi, "Characteristics of nondegenerate four-wave mixing in electroabsorption modulator", Appl. Phys. Lett., **85**, 869 (2004).

[13] L. Hou, R. Dylewicz, M. Haji, P. Stolarz, B. Qiu, A. C. Bryce, "Monolithic 40 GHz passively mode-locked AlGaInAs/InP 1.55 μm MQW laser with surface-etched distributed Bragg reflector", IEEE Photon. Technol. Lett. **22**, 1503 (2010).

[14] L. Hou, M. Haji, R. Dylewicz, B.C. Qiu, A. Catrina Bryc, "10 GHz mode-locked extended cavity laser integrated with surface-etched DBR fabricated by Quantum Well Intermixing," IEEE Photon. Technol. Lett. **23**, 82(2011).

[15] M. Blez, C. Kazmierski, D. Mathoorasing, M. Quillec, M. Gilleron, H. Nakajima and B. Sennage, "High speed ultralow chirp 1.55 μm MBE grown GalnAs/AIGalnAs MQW DFB lasers", Electron. Lett. **27,** 93 (1992).

[16] S. Spiessberger , M. Schiemangk, A. Wicht, H. Wenzel, O. Brox, and G. Erbert, "Narrow linewidth DFB lasers emitting near a wavelength of 1064 nm", J. Lightwave Technol. **28**, 2611 (2010).